crystals

MDPI

Article

Growth, Structure, and Spectroscopic Properties of a Disordered Nd:$SrLaGaO_4$ Laser Crystal

Shanshan Fang [1,2], Ling Liang [1,2], Wei Wang [1,2], Yiyang Lin [1,2], Yijian Sun [1,2,*], Guoliang Gong [1,2], Chaoyang Tu [1] and Herui Wen [1]

[1] School of Chemistry and Chemical Engineering, Jiangxi Provincial Key Laboratory of Functional Molecular Materials Chemistry, Jiangxi University of Science and Technology, Ganzhou 341000, China
[2] National Rare Earth Functional Material Innovation Center, Ganzhou 341000, China
* Correspondence: sunyijian@jxust.edu.cn

Abstract: A disordered Nd:$SrLaGaO_4$ (Nd:SLG) laser crystal was successfully grown via the Czochralski (CZ) technique. The crystal structure, refractive index, polarized absorption spectra, and stimulated emission spectra were measured. The spectroscopic properties were studied intensively with the Judd–Ofelt (J-O) theory. The maximum absorption cross sections of π- and σ-polarization at 806 nm were calculated to be 3.73×10^{-20} and 4.05×10^{-20} cm^2, corresponding to FWHMs of 6.00 and 6.10 nm, respectively. The maximum emission cross sections of π- and σ-polarization at 1076 nm were 3.97×10^{-20} and 4.12×10^{-20} cm^2, with FWHMs of 30.21 and 19.44 nm, respectively. The decay life of the Nd^{3+}:$^4F_{3/2}$ energy level was fitted to be 0.152 ms, and the fluorescence quantum efficiency was 72.72%. The inhomogeneous broadening in spectra benefiting from the disordered structure indicates the Nd:SLG crystal is a promising gain medium for ultrafast laser and tunable laser generations in the near infrared region.

Keywords: Nd:$SrLaGaO_4$; disordered crystal; J-O theory; spectroscopic properties

Citation: Fang, S.; Liang, L.; Wang, W.; Lin, Y.; Sun, Y.; Gong, G.; Tu, C.; Wen, H. Growth, Structure, and Spectroscopic Properties of a Disordered Nd:$SrLaGaO_4$ Laser Crystal. *Crystals* **2024**, *14*, 174. https://doi.org/10.3390/cryst14020174

Academic Editor: Ludmila Isaenko

Received: 28 December 2023
Revised: 1 February 2024
Accepted: 4 February 2024
Published: 9 February 2024

1. Introduction

Ultrafast and tunable lasers show extensive applications in intelligent processing [1], communication and remote sensing [2], national defense and military [3], medical beauty, and scientific research [4] because of the high pulse energy, high peak power, and short duration. In recent years, crystals with disordered structures have attracted extensive attention for ultrafast and tunable lasers gain media due to the wide emission band [5–8]. The random distribution of cations with different valences in the same lattice position leads to the disordered distribution of the lattice field, which leads to the uneven broadening of absorption and emission spectra [9,10].

For a 1.0 μm wavelength laser, Nd^{3+}-doped laser crystals exhibit high pump efficiency and a low threshold due to the long upper\-level lifetime, large emission cross section, and no reabsorption loss of Nd^{3+} ions [8–13]. In recent years, many novel Nd^{3+}-doped crystals have been reported to realize ultrashort or Q-switched pulsed lasers, such as Nd:$GdSr_3(PO_4)_3$ [5], Nd:$LaMgAl_{11}O_{19}$ [6], Nd:$LuYPO_4$ [8], Nd:Ca(Y, Gd)AlO_4 [9], and Nd:$GdScO_3$ [14]. Among those crystals, disordered aluminate (gallate) crystals present excellent thermal properties and spectral broadening, which is always regarded as the potential gain medium for high-power and ultrafast lasers [1,3,9,15–20]. In 2018, Lin et al. reported a new Nd:$Gd_2SrAl_2O_7$ crystal and achieved 1.55 W continuous-wave laser output at 1080 nm [16]. In 2020, Xu et al. demonstrated a high repetition rate passively Q-switched laser in the Nd:$SrAl_{11}O_{19}$ (Nd:SRA) crystal, corresponding to a high repetition rate of 201 kHz, a Q-switched pulse width of 346 ns, a peak power of 1.87 W, and a single pulse energy of 0.65 μJ [17]. Jia et al. reported spectroscopy and laser performance in a novel disordered crystal of Nd^{3+}-doped $CaYAl_3O_7$ (CYAM) [18]. In 2021, Xu et al. reported a

diode-pumped continuous-wave Nd:$CaLaGa_3O_7$ laser with a range of about 22 nm [19]. In 2023, Xu et al. successfully grown a disordered Nd:$CaGdAl_3O_7$ crystal via the optical floating zone method and made a detailed analysis of the disordered structure and the broad spectroscopic properties [20].

The $ABCO_4$ family crystallizes in the K_2NiF_4 tetragonal structure with a space group of I_4/mmm, has a complex and disordered lattice field, which causes a large inhomogeneous broadening of absorption and emission spectra. In general, rare-earth-doped $CaYAlO_4$, $CaGdAlO_4$, and $SrLaAlO_4$ laser crystals have been widely studied in ultrafast and tunable laser fields [7,9,15,21–24]. In 2016, Liu et al. reported a stable 458 femtosecond continuous-wave mode-locked pulse in the Nd:$SrLaAlO_4$ crystal at 1077.9 nm with an average power output of 520 mW [21]. In 2022, Yang et al. achieved a continuous single-frequency tunable laser at 1.08 μm with a tuning range of 60.72 GHz in the Nd:$CaYAlO_4$ crystal [24]. Chen et al. first reported a Nd-doped tunable laser beyond 1100 nm in the mixed Nd:CYGA crystal, where Gd^{3+} ions were introduced into the $CaYAlO_4$ crystal [15]. Among the $ABCO_4$ single crystal family, $SrLaGaO_4$ (SLG) crystal has been widely studied as a substrate material with epitaxial growth method for high-temperature superconducting thin films due to the low dielectric loss and good lattice matching with various superconducting coppers such as $YBa_2Cu_3O_{7-x}$ [25]. The disordered environment formed by the random distribution of Sr^{3+} ions and La^{3+} ions may lead to a strong inhomogeneous broadening of the absorption and emission spectra. Thus, one could expect that the $SrLaGaO_4$ crystal may also be a potential laser material. However, research on rare-earth-doped SLG laser crystals is still limited. Dabkowski reported the Czochralski crystal growth of pure $SrLaGaO_4$ crystal in 1993 [26]. A brief study on the structure and absorption spectra properties of Nd:$SrLaGaO_4$ was first reported by Ryba-Romanowski in 1996 [27]. While there has been no systematic research on Nd:$SrLaGaO_4$ as a near-infrared laser gain medium in recent decades, it is necessary to study the crystal structure, refractive index, polarized absorption spectra, stimulated emission spectra, and decay life in detail to evaluate ultrafast and tunable laser performance in Nd:$SrLaGaO_4$. Nevertheless, these requirements have not been addressed thus far.

In this work, a detailed study on the Nd:$SrLaGaO_4$ crystal for ultrafast and tunable lasers in the near infrared region was presented. The pure and Nd-doped SLG crystals were grown by the Czochralski method in a rich Ga condition. The crystal structure was studied based on the Rietveld XRD refinement. The refractive index dispersion equations were fitted by the least squares method. The polarized spectroscopic properties and the fluorescence lifetime were studied intensively. Compared to the spectroscopic parameters of some other Nd^{3+}-doped laser crystals, the broadening spectra characteristics indicated that Nd:SLG crystals are a good material for ultrafast and tunable lasers at 1.0 μm.

2. Experiment

In this paper, pure SLG and 1% Nd:SLG crystals were successfully grown by the Czochralski method in a rich Ga condition. The raw materials $SrCO_3$, La_2O_3, Ga_2O_3, and Nd_2O_3 with a purity of 4N were used without any treatment. According to a report in [26], SLG crystal grown in rich Ga conditions shows better crystallinity. Thus, more $SrCO_3$ and Ga_2O_3 and less La_2O_3 were weighed than the stoichiometric composition for the polycrystalline synthesis process in this work. After grinding and mixing the raw materials evenly, the plates were pressed and then sintered at 1250 °C for 3 days in a muffle furnace for high-temperature solid-phase reaction. Before crystal growth, the polycrystalline phase was proved to be pure by X-ray diffraction (XRD). For crystal growth, the polycrystalline raw material was loaded into a Φ60 mm iridium crucible with nitrogen protection. A c-cut pure SLG crystal was used as the seed for Nd:SLG crystal growth. During the crystal growth, the pulling rate was 1–2 mm/h and the rotation rate was 6–10 rpm/min, respectively. After crystal growth, in order to relieve the thermal stress, the crystal was cooled to room temperature slowly with a speed of 5–35 K/h. The dimension of the as-grown 1.0 at.%Nd:SLG crystal is about Φ25 mm × 35 mm. After annealing at 1000 °C

for 48 h in a N_2 (98%)–H_2 (2%) atmosphere, the Nd:SLG crystal changed from atrovirens to purplish brown, indicating a color center defect in the crystal. Although treated in a reducing atmosphere, the color of the Nd:SLG crystal is still different from the usual Nd^{3+}-doped laser crystals. There are some other color center defects in the Nd:SLG crystal compared with common O^- defects in the $ABCO_4$ family, which will be of great interest in further study.

The crystal structures were identified by powder XRD (Rigaku Miniflex 600 diffractometer, Rigaku, Tokyo, Japan). The patterns were collected in the range of 10–80° with a scanning speed of 2○/min. The concentration of the Nd^{3+} ion in the Nd:SLG crystal was determined by inductively coupled plasma atomic emission spectrometry (ICP-AES, TPS-7000). A fully automatic high-precision refractometer (UV VIS SWIR IR 3-12 (Trioptics, Hamburg, Germany)) was used to test the refractive index. The crystallography c-axis of the Nd:SLG crystal was oriented by an X-ray direction finder (YX-Z). A small slice with a thickness of 2 mm was cut for polarized spectra. The incident surface was parallel to the c-axis and polished. Polarized absorption spectra were measured with a Perkin-Elmer UV-visible-near infrared spectrometer (Lambda-950, Perkin-Elmer, Waltham, MA, USA) in the range of 300–1000 nm. The polarized fluorescence spectra and fluorescence decay curve were recorded on an FLS920 fluorescence spectrometer (Edinburgh, Livingston, UK), with the xenon lamp as an excitation source. All the tests were recorded at room temperature.

3. Results and Discussion

3.1. Crystal Structure and Segregation

The structure of the Nd:SLG crystal was identified by powder XRD. As shown in Figure 1, all the diffraction peaks match well with the standard card (PDF#24-1208) with tetragonal phase, further indicating that the Nd^{3+} ions can be doped into the SLG host lattice by replacing the La^{3+} ions without any obvious variations to the host structure.

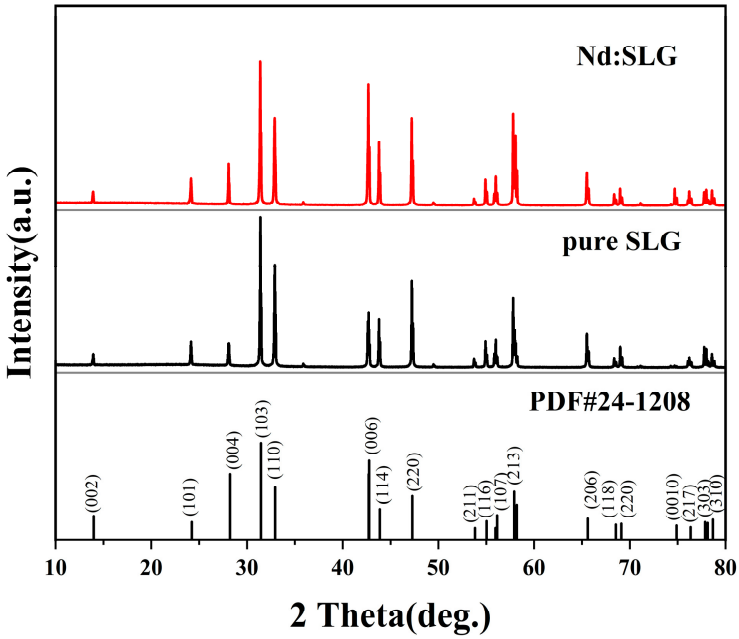

Figure 1. The XRD patterns of the as-grown Nd:SLG crystal.

Based on the Rietveld XRD refinement, the structure of the Nd:SLG crystal was further studied in Figure 2. As shown in Figure 2a, the observed and calculated diffraction patterns match well with each other, revealing that the Nd:SLG crystal possesses a pure single tetragonal phase with a space group of I_4/mmm. The lattice parameters of the Nd:SLG crystal are calculated to be a = b = 3.84146 Å and c = 12.6813 Å. Because of the Nd^{3+} ions doping with a smaller cation radius than La^{3+} ions, the lattice parameters of the

Nd:SLG crystal are slightly smaller than those of the pure SLG crystal (PDF #24-1208). The corresponding refined crystal structure parameters are presented in Table 1. Figure 2b displays a schematic structure of the Nd:SLG crystal. It can be seen that the Nd:SLG crystal is built up from GaO_6 layers, between which Nd^{3+} ions, Sr^{3+} ions, and La^{3+} ions are distributed randomly with C_{4v} symmetry.

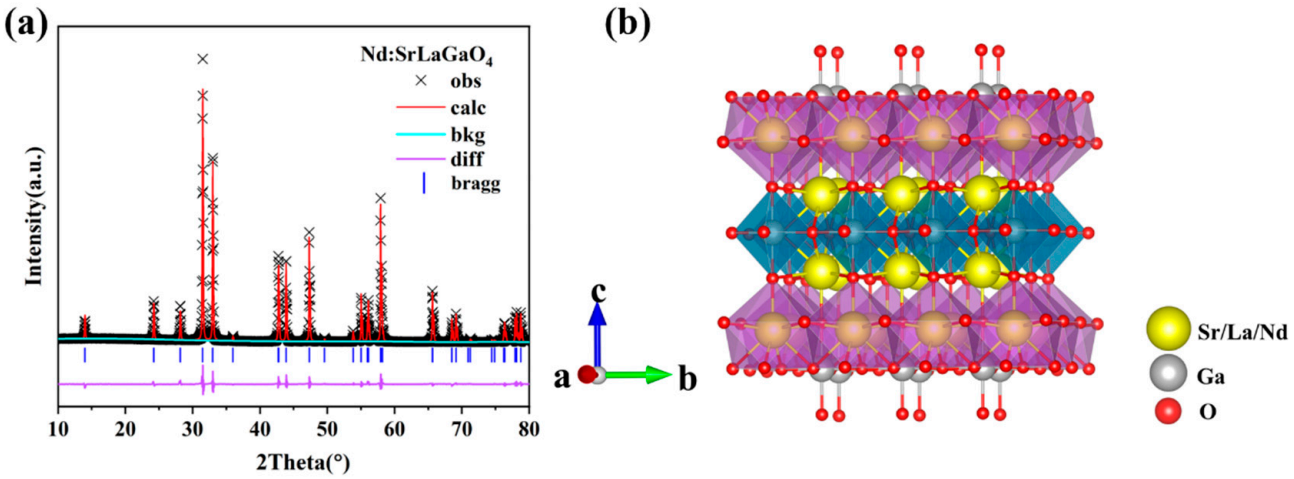

Figure 2. (**a**) Rietveld XRD refinement results and (**b**) structure of the Nd:SLG crystal.

Table 1. Crystal structure parameters of Nd:SLG obtained by Rietveld full-profile refinement.

Name	X	Y	Z	Wyckoff Site	Uiso
Sr_1	0	0	0.3588	4e	0.00425
La_1	0	0	0.3588	4e	0.00992
Ga_1	0	0	0	2a	0.01715
O_1	0	0	0.1680	4e	0.00914
O_2	0	0.5	0	4c	0.01923
Nd_6	0	0	0.3588	4e	0.00250

FirsCell parameters: a = b = 3.84146 Å, c = 12.6813 Å, $\alpha = \beta = \gamma = 90°$. Cell volume: V = 187.135 $Å^3$, space group: tetragonal, I_4/mmm (139). Density: $\rho = 6.398$ g/cm^3. Reliability factors (R-factor): GOF = 1.62, R_{wp} = 7.743%.

The segregation coefficient is an important factor for laser crystals because it affects structure uniformity and laser output efficiency. With the help of the ICP-AES test, the lattice concentration of Nd^{3+} ions was calculated to be 1.27×10^{-20} ions/cm^3. The corresponding segregation coefficient was calculated to be 0.48, which was similar to the $Nd:LuYPO_4$ crystal [8].

3.2. Refractive Index

Refractive index is an important parameter for laser gain mediums. Since SLG crystal belongs to the tetragonal structure and uniaxial optical crystals, the minimum deviation technique with a right-angle prism sample, as shown in the inset in Figure 3, is used for the refractive index measurements of SLG crystal. The incident light must be perpendicular to the optic principal c-axis. With the help of a polarizer, o-light and e-light can be separated behind the prism. Based on the included angle to the incident light, n_o and n_e can be calculated, respectively. Table 2 shows the crystal refractive index test data. Seven test points with different wavelengths were selected, ranging from 546.07 nm to 1013.98 nm.

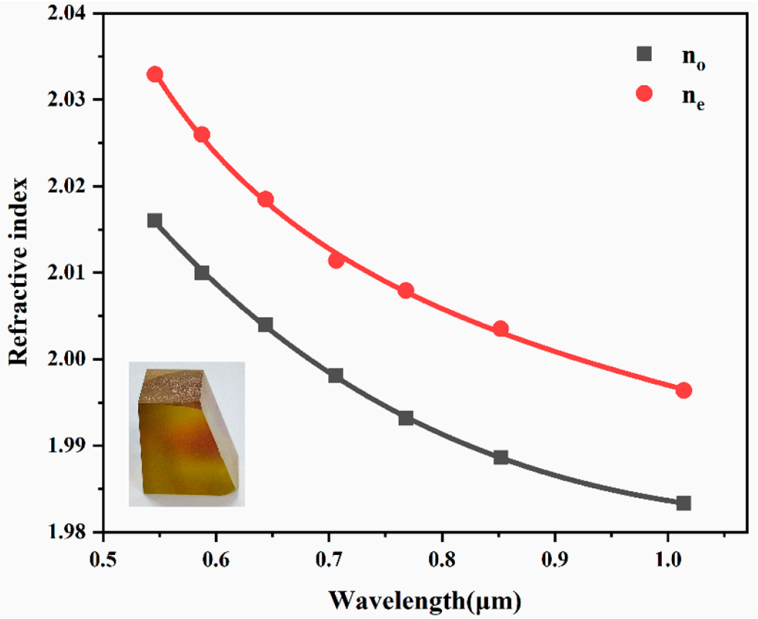

Figure 3. The refractive index dispersion curve of SLG crystal. The inset is the optical prism sample.

Table 2. The refractive index test data of the SLG crystal.

λ (nm)	Refractive Index	
	n_o	n_e
546.0750	2.0159794	2.0329168
587.5620	2.0099844	2.0259665
643.8470	2.0039589	2.0184998
706.5190	1.9980698	2.0114033
768.1943	1.9931367	2.0079149
852.1100	1.9886278	2.0034969
1013.9800	1.9833680	1.9963757

As shown in Figure 3, the refractive index dispersion equations (Sellmeier) are fitted by the least squares method as follows:

$$n_o^2 = -9.28518 + \frac{13.17287\lambda^2}{\lambda^2 - 0.00401} - 0.00615\lambda^2$$

$$n_e^2 = -7.16368 + \frac{11.09283\lambda^2}{\lambda^2 - 0.00537} - 0.00074\lambda^2$$

where λ represents the wavelength and the unit is μm. It can be seen that the SLG crystal is a positive uniaxial crystal ($n_o < n_e$). The fitted refractive index dispersion equation is in good agreement with the actual measured value. The fitted refractive index dispersion equations can be used in the spectra and Judd–Ofelt (J-O) theory analyses next.

3.3. Absorption Spectra and Judd–Ofelt (J-O) Theory Analyses

Figure 4 shows the π- and σ-polarized absorption spectra of the Nd:SLG crystal at room temperature in the range of 500–1000 nm. All the absorption peaks have been marked. The peaks are located at 529, 589, 684, 751, 806, and 879 nm, corresponding to the transition of Nd^{3+} ions from the ground state $^4I_{9/2}$ to the excited state $^4G_{9/2} + {}^4G_{7/2} + {}^2K_{13/2}$, $^4G_{5/2} + {}^2G_{7/2}$, $^4F_{9/2}$, $^4S_{3/2} + {}^2H_{7/2}$, $^4F_{5/2} + {}^2H_{9/2}$, and $^4F_{3/2}$. Due to the absorption of color center defects, a broad absorption peak instead of the characteristic absorption peak of Nd^{3+} ions appeared at wavelengths shorter than 500 nm. The characteristic absorption peak of Nd^{3+} ions located at 806 nm, corresponding to the transition $^4I_{9/2} \rightarrow {}^4F_{5/2} + {}^2H_{9/2}$, is well

matched with the emission band of commercial AlGaAs laser diodes. The absorption cross section can be calculated using the following formula:

$$\sigma_{\mathrm{abs}}(\lambda) = \frac{2.303 \times \mathrm{OD}(\lambda)}{N_0 \times \mathrm{L}}$$

where $\mathrm{OD}(\lambda)$ is the absorption optical density, N_0 is the lattice concentration (the number of Nd^{3+} ions per cubic centimeter), and L is the thickness of the sample. The maximum absorption cross sections of the Nd:SLG crystal for π-polarization and σ-polarization at 806 nm are calculated to be 3.73×10^{-20} cm^2 and 4.05×10^{-20} cm^2, which is larger than the disordered Nd:$SrLaAlO_4$ (2.45×10^{-20} cm^2) [21], Nd:$SrLaGa_3O_7$ (1.99×10^{-20} cm^2) [28], Nd:$SrAl_{12}O_{19}$ crystals (0.21×10^{-20} cm^2 [π], 2.08×10^{-20} cm^2 [σ]) [29], and comparable to Nd:$CaYAl_3O_7$ (3.51×10^{-20} cm^2 [π], 5.34×10^{-20} cm^2 [σ]) [18] and $CaGdAl_3O_7$ (3.78×10^{-20} cm^2) [20] crystals. The corresponding full width at half maximums (FWHMs) around 806 nm are 6.00 nm and 6.10 nm, respectively, which far exceed the Nd:YAG and Nd:YVO_4 crystals and are also close to some commonly disordered crystals such as Nd:$CaYAlO_4$ (5 nm) [23] and Nd:$CaGdAlO_4$ (5 nm) [22]. The large absorption cross sections and wide absorption bands resulting from the disordered structure of the crystal suggest that the Nd:SLG crystal is suitable for commercial AlGaAs laser diode pumping, which is beneficial to pump absorption efficiency and light-to-light conversion efficiency in laser operation.

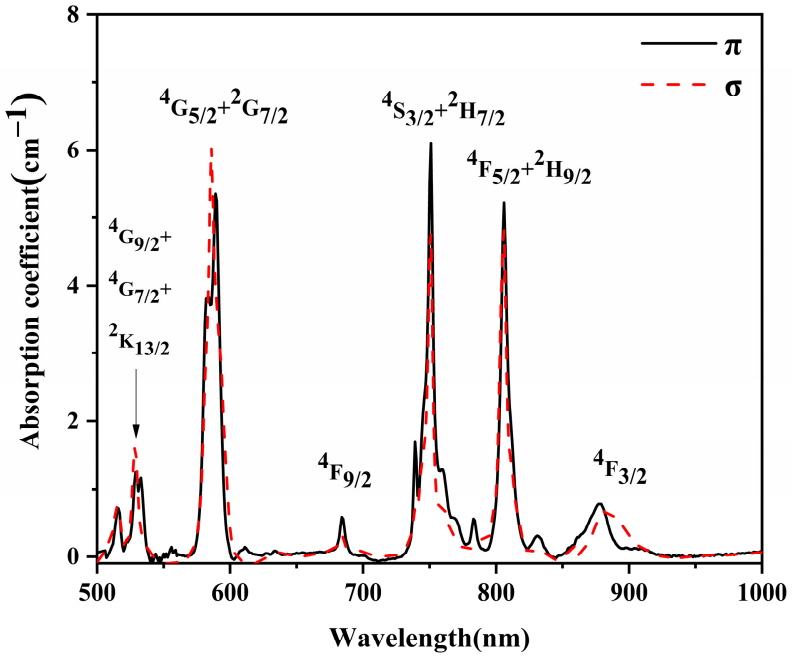

Figure 4. The polarized absorption spectra of the Nd:SLG crystal at 500–1000 nm.

The J-O theory is widely applied for systematic spectroscopic analysis of some rare earth-doped optical materials [8,20]. Based on the polarized absorption spectra, some important spectral parameters of the Nd:SLG crystal can be estimated, such as the oscillator strength, the J-O intensity parameters, the transition branching ratio, and the radiative lifetime.

The experimental absorption line intensity S_{exp} is calculated through absorption spectroscopy using the following equation:

$$S_{exp} = \frac{9n}{(n^2+2)^2} \cdot \frac{3hc(2J+1)}{8\pi^3 e^2 \bar{\lambda} N_0} \int \alpha(\lambda) d\lambda$$

where e, n, h, and c are the electron charge, refractive index, Planck constant, and speed of light, respectively. J is the initial total angular momentum quantum number, $\overline{\lambda}$ is the mean wavelength, N_0 is the concentration of the Nd^{3+} ion, and $\alpha(\lambda)$ is the absorption coefficient at the wavelength of λ.

Meanwhile, the calculated line intensity S_{cal} is obtained by the following equation:

$$S_{cal} = \sum_{2,4,6} \Omega_\lambda |\langle 4f^n \psi J \| U^{(t)} \| 4f^n \psi^* J^* \rangle|^2$$

where the Ω_λ (λ = 2,4,6) are the J-O strength parameters, and $U^{(t)}$ (t = 2,4,6) are the squared matrix elements. Then all the experimental absorption line intensity S_{exp} and the calculated line intensity S_{cal} are listed in Table 3. The results show that the calculated oscillator strengths coincide well with the measured ones.

Table 3. The oscillator strength of the Nd:SLG crystal.

Nd^{3+} $^5I_8 \rightarrow$	σ-Polarized			π-Polarized		
	λ (nm)	S_{exp}	S_{cal}	λ (nm)	S_{exp}	S_{cal}
		10^{-20} cm^2			10^{-20} cm^2	
$^4G_{9/2} + {}^4G_{7/2} + {}^2K_{13/2}$	529	7.059	6.032	529	6.099	4.673
$^4G_{5/2} + {}^2G_{7/2}$	586	18.68	18.74	589	20.93	21
$^4F_{9/2}$	684	1.08	0.549	684	0.616	0.633
$^4S_{3/2} + {}^2H_{7/2}$	751	7.239	6.627	751	9.355	8.583
$^4F_{5/2} + {}^2H_{9/2}$	806	6.126	7.086	806	5.755	6.922
$^4F_{3/2}$	883	2.909	2.653	879	1.629	1.2
$RMS\Delta S$		0.293			0.243	

The root-mean-square deviation ($RMS\Delta S$) is calculated by the following equation:

$$RMS\Delta S = \sqrt{\frac{\sum_{J'} \left(S_{exp} - S_{cal}\right)^2}{N - 3}}$$

where N is the number of absorption bands used in the analysis. The root mean square deviation ($RMS\Delta S$) of π-polarized and σ-polarized strength parameters are 2.432 × 10^{-21} cm^2 and 2.932 × 10^{-21} cm^2, which confirms the agreement between the experimental and theoretical data within the error tolerance.

As listed in Table 4, the J-O strength parameters $\Omega_{2,4,6}$ are calculated as Ω_2 (3.28 × 10^{-20} cm^2), Ω_4 (2.97 × 10^{-20} cm^2), and Ω_6 (3.61 × 10^{-20} cm^2) by the formula $\Omega_{\text{eff}} = (2\Omega_\sigma + \Omega_\pi)/3$. The large Ω_2 indicates that the crystal possesses lower symmetry and stronger covalent properties, further proving its disordered structure. The value of Ω_4/Ω_6 of 0.82, representing the spectroscopic quality factor, is comparable with that of Nd:YVO_4 (0.8) [30] and Nd:$CaYAlO_4$ (0.95) [23], which indicates highly feasible laser generation in the Nd:SLG crystal.

Table 4. The J-O intensity parameters of Nd^{3+}-doped crystals.

Crystal	$\Omega_{2,4,6}$ (10^{-20} cm^2)				Ref.
	Ω_2	Ω_4	Ω_6	Ω_4/Ω_6	
Nd:SLG	3.28	2.97	3.61	0.82	This work
Nd:YAG	0.62	1.70	5.76	0.29	[31]
Nd:$SrLaGa_3O_7$	1.28	5.01	1.95	2.57	[28]
Nd:$CaLaGa_3O_7$	5.804	10.586	3.443	3.07	[32]
Nd:YVO_4	5.88	4.08	5.11	0.80	[30]
Nd:$CaYAlO_4$	2.19	8.16	8.57	0.95	[23]

Table 5 shows the radiative transition rate, fluorescence branching ratio β, and radiation lifetime τ_{rad}. The transition $^4F_{3/2} \rightarrow {}^4I_{11/2}$ has the largest fluorescence branching ratio of 48.88%, indicating the most likely emission at 1.0 μm. The radiative lifetime of the crystal is fitted to be 0.21 ms.

Table 5. The radiative transition rates A_{ed}, branching ratios β, and radiative lifetime τ_{rad} of Nd:SLG.

Transition		λ (nm)	A_{ed} (s^{-1})	β (%)	τ_{rad} (ms)
$^4F_{3/2} \rightarrow$					0.21
	$^4I_{15/2}$	1852	23.99864	0.51	
	$^4I_{13/2}$	1333	465.4819	9.95	
	$^4I_{11/2}$	1053	2290.509	48.95	
	$^4I_{9/2}$	881	1898.881	40.58	

3.4. Fluorescence Spectra

Figure 5 shows the polarized emission spectra of the Nd:SLG crystal, ranging from 820 to 1450 nm under 806 nm excitation. Three peaks with a central wavelength of 896, 1076, and 1360 nm are marked. The strongest peak at 1076 nm, corresponding to the transition of $^4F_{3/2} \rightarrow {}^4I_{11/2}$, is also consistent with the JO theoretical analysis. Moreover, the relative intensity of the peaks for π-polarization and σ-polarization is very similar. While the maximum emission of σ-polarization is about five times greater than that of π-polarization due to the anisotropy of the Nd:SLG crystal, the stimulated emission cross sections at 1076 nm are calculated as 3.97×10^{-20} cm^2 for π-polarization and 4.12×10^{-20} cm^2 for σ-polarization by the following formula:

$$\sigma_{em}(\lambda) = \frac{\lambda^5 I(\lambda)\beta}{8\pi c n^2 \cdot \tau_r \int I(\lambda)\lambda d\lambda}$$

where β is the fluorescence branching ratio, λ is the emission wavelength, $I(\lambda)$ is the fluorescence intensity, c is the speed of light in vacuum, n is the refractive index, τ_r is the radiative lifetime, and $\frac{I(\lambda)}{\int I(\lambda)\lambda d\lambda}$ is the normalized line shape function of the emission spectrum. Because of the largest fluorescence branching ratio of $^4F_{3/2} \rightarrow {}^4I_{11/2}$ transition, the stimulated emission cross sections at 1076 nm are significantly larger than those of the emissions around 0.9 μm and 1.3 μm. Compared with some known disordered crystals, the emission cross sections of the Nd:SLG crystal at 1076 nm are a little larger than those of the Nd:$SrGdGa_3O_7$ (2.00×10^{-20} cm^2) [33] and comparable to those of the Nd:$CaGdAl_3O_7$ (4.94×10^{-20} cm^2) [20]. The corresponding FWHMs of the Nd:SLG crystal are 30.21 and 19.44 nm for π-polarization and σ-polarization, which is wider than most of the disordered crystals, such as Nd:$CaYAl_3O_7$ crystal (14.4 nm [σ]) [18], Nd:$CaYAlO_4$ crystal (12 nm [σ]) [23], and Nd:$SrLaGa_3O_7$ crystal (16.9 nm) [28]. The appropriate emission cross-sections and large emission bandwidth indicate a potential laser operation beyond 1.1 μm and are beneficial for wavelength-tunable and ultrashort pulse solid-state laser generations.

Figure 6 presents the fluorescence decay lifetime of the Nd^{3+}:$^4F_{3/2}$ energy level at the wavelength of 1076 nm under 806 nm excitation. The fluorescence lifetime is fitted to be 0.152 ms by a single exponential and linear function fit, which is longer than that of Nd:YVO_4 (0.084 ms) [34] and comparable to Nd:$CaYAlO_4$ (0.129 ms) [23], Nd:$CaGdAlO_4$ (0.123 ms) [22], and Nd:$SrLaAlO_4$ (0.138 ms) [35]. Due to the phonon relaxation between the host and Nd^{3+} ions, the fluorescence lifetime τ_f is always smaller than that of the calculated radiation lifetime τ_{rad} by the J-O theory. According to the formula $\eta = \tau_f/\tau_{rad}$, the fluorescence quantum efficiency η can be calculated as 72.72%. The long fluorescence lifetime and large fluorescence quantum efficiency reveal that the Nd:SLG crystal is suitable for high-power solid-state laser generation.

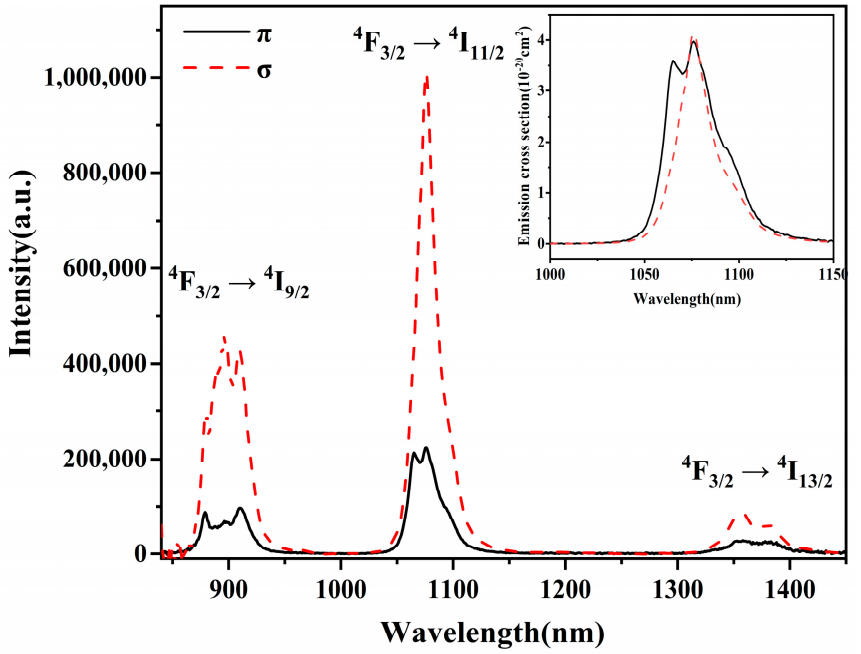

Figure 5. The polarized emission spectra of the Nd:SLG crystal under 806 nm excitation; the inset is the emission cross-section of the Nd:SLG crystal around 1.0 μm.

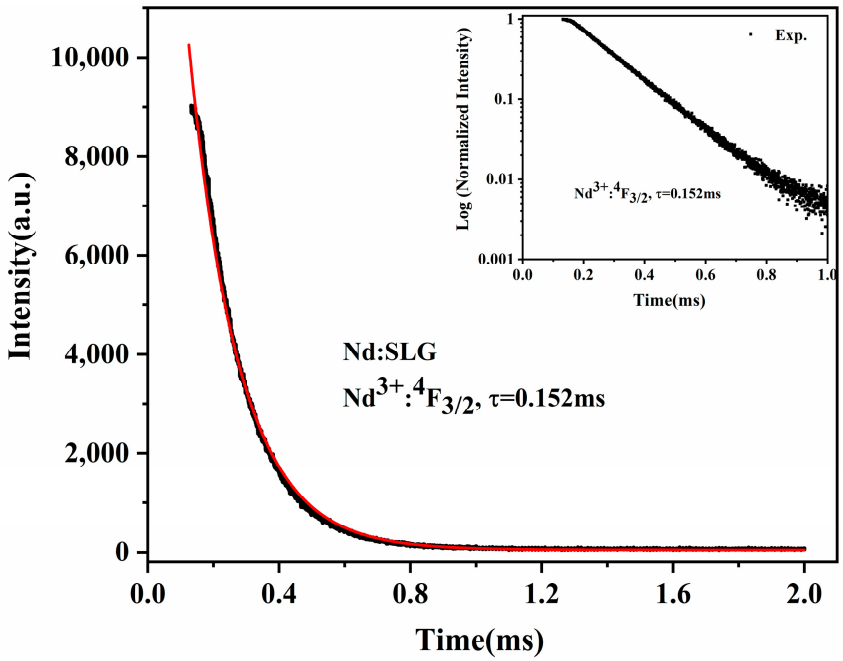

Figure 6. Fluorescence decay curves of the Nd:SLG crystal for the Nd^{3+}: $^4F_{3/2}$ energy level.

Table 6 presents a brief comparison of Nd-doped spectroscopic properties between the common crystals and some disordered laser crystals. Compared with the spectroscopic parameters of the typical Nd:YAG and Nd:YVO_4 crystals, the disordered crystals always present broadening spectra characteristics, which is desirable for the generation of wavelength-tunable lasers and ultrashort pulse lasers. The large emission bandwidth, the appropriate emission cross-section, and the long fluorescence lifetime also indicate the Nd:SLG crystal as an effective gain material for 1.0 μm ultrafast and tunable lasers.

Table 6. A comparison of the Nd-doped spectroscopic properties between the common crystals and some disordered laser crystals.

Crystal	λ_{abs} (nm)	σ_{abs} (10^{-20} cm^2)	*FWHM* (nm)	λ_{em} (nm)	σ_{em} (10^{-20} cm^2)	*FWHM* (nm)	τ_f (μs)	Refs.
YAG	808	7.3	1	1064	28	0.8	230	[36,37]
YVO_4	808.7(π)	38.7(π)	1.9(π)	1066(σ)	29.5(σ)	3.5(σ)	84.1	[34]
$CaYAlO_4$	806(σ)	9.7(σ)	5(σ)	1080(σ)	10.44(σ)	12(σ)	129	[23]
$CaGdAlO_4$	809(π) 809(σ)	6.8(π) 7.5(σ)	4(π) 5(σ)	1067(π) 1068(σ)	12.5	18(π) 11(σ)	123	[22]
$SrLaAlO_4$	808(σ) 808(π)	2.44(σ) 2.43(π)	17(σ) 17(π)	1075(σ) 1065–1078(π)	3.8(σ) 5.2–5.5(π)	/ 34(π)	138	[35]
$CaYAl_3O_7$	808(σ) 808(π)	5.34(σ) 3.51(π)	20.2(σ) 20.2(π)	1062(σ) 1062(π)	4.55(σ) 5.97(π)	14.4(σ) 14(π)	261	[18]
$CaGdAl_3O_7$	808.5	3.78	19.3	1061.6	4.94	12.7	260.7	[20]
$CaLaGa_3O_7$	808(σ) 808(π)	1.34(σ) 3.18(π)	10(σ) 16(π)	1061(σ) 1061(π)	6.9(σ) 7.23(π)	27.8(σ) 18.8(π)	250	[32]
$Gd_2SrAl_2O_7$	808(σ) 807.5(π)	11.84(σ) 13.7(π)	3.4(σ) 3.3(π)	1080 1080	12.7(σ) 15(π)	12.5(σ) 5.1(π)	118	[16]
$SrLaGaO_4$	806(σ) 806(π)	4.05(σ) 3.73(π)	6.1(σ) 6(π)	1076(σ) 1076(π)	4.12(σ) 3.97(π)	19.44(σ) 30.21(π)	152	This work

4. Conclusions

In short, a disordered Nd:$SrLaGaO_4$ crystal had been successfully grown by the Czochralski method in a rich Ga condition. The crystal structure, refractive index, polarized absorption spectra, and emission spectra were studied in detail.

1. XRD was used to verify the unchanged tetragonal structure of the Nd^{3+}-doped crystal. The Nd^{3+}, Sr^{3+}, and La^{3+} ions were distributed randomly with C_{4v} symmetry. The calculated lattice concentration and effective segregation coefficient of Nd^{3+} ions were 1.27×10^{-20} ions/cm^3 and 0.48.
2. The refractive index of the Nd:SLG crystal was measured by the minimum deviation technique with a right-angle prism sample. The refractive index dispersion equation was fitted by the least squares method. The results reveal that the SLG crystal is a positive uniaxial crystal.
3. The polarized absorption spectra of the Nd:SLG crystal were measured at room temperature. The maximum absorption cross sections of π- and σ-polarization at 806 nm were 3.73×10^{-20} and 4.05×10^{-20} cm^2, and the corresponding FWHMs were 6.00 and 6.10 nm, respectively. Based on the J-O analysis, the $^4F_{3/2} \rightarrow {}^4I_{11/2}$ transition around 1.0 μm had the largest fluorescence branch ratio of 48.88%.
4. The stimulated emission cross sections at 1076 nm were calculated as 3.97×10^{-20} cm^2 for π-polarization and 4.12×10^{-20} cm^2 for σ-polarization, and the corresponding FWHMs were 30.21 and 19.44 nm, respectively. The decay lifetime of the Nd^{3+}:$^4F_{3/2}$ energy level of Nd^{3+} ions at 1076 nm was fitted to 0.152 ms by a single exponential.

The broadening spectra characteristics resulting from the disordered crystal structure, as well as the appropriate emission cross-section and the long fluorescence lifetime, show the Nd:SLG crystal to be a good gain material for ultrafast and tunable lasers at 1.0 μm.

Author Contributions: Methodology, Y.S.; validation, S.F. and Y.L.; formal analysis, S.F., L.L., W.W., Y.S., G.G. and C.T.; investigation, S.F. and Y.S.; data curation, S.F., W.W., Y.L. and Y.S.; writing—original draft, S.F. and L.L.; writing—review and editing, Y.S., G.G., C.T. and H.W. All authors have read and agreed to the published version of the manuscript.

Funding: This work has been supported by the National Natural Science Foundation of China (No. 12104194, 11764014), the Key Research and Development Project of Jiangxi Province (20232BBE50030), the Natural Science Foundation of Jiangxi Province (20212BAB213015), the Jiangxi

Provincial Key Laboratory of Functional Molecular Materials Chemistry (20212BCD42018), and Ganzhou Science and Technology Plan Project (2023CYZ27831, 2022XM079296).

Data Availability Statement: The original contributions presented in the study are included in the article; further inquiries can be directed to the corresponding author.

Conflicts of Interest: The authors declare no conflicts of interest.

References

1. Wei, M.; Cheng, T.; Dou, R.; Zhang, Q.-L.; Jiang, H. Superior performance of a 2 kHz pulse Nd:YAG laser based on a gradient-doped crystal. *Photonics Res.* **2021**, *9*, 1191–1196. [CrossRef]
2. Li, G.; Zhou, Q.; Xu, G.; Wang, X.; Han, W.; Wang, J.; Zhang, G.; Zhang, Y.; Yuan, Z.; Song, S.; et al. Lidar-radar for underwater target detection using a modulated sub-nanosecond Q-switched laser. *Opt. Laser Technol.* **2021**, *142*, 107234. [CrossRef]
3. Qian, C.; Jiang, Y.; Wu, Y.; Yue, B.; Yan, S.; Lu, Z. The comparison of the efficacy and safety of fractional 1064 nm Nd:YAG picosecond laser and nonablative fractional 1565 nm laser in the treatment of enlarged pores: A prospective split-face study. *Lasers Surg. Med.* **2023**, *55*, 169–177. [CrossRef]
4. Yun, Q.; Song, B.; Pei, Y. Modeling the impact of high energy laser weapon on the mission effectiveness of unmanned combat aerial vehicles. *IEEE Access* **2020**, *8*, 32246–32257. [CrossRef]
5. Wu, G.; Bai, L.; Yu, P.; Fan, M.; Sun, L.; Li, Y.; Yu, F.; Wang, Z.; Zhao, X. Growth, optical, and spectroscopic properties of pure and Nd^{3+}-doped $GdSr_3(PO_4)_3$ crystals with disordered structure. *Inorg. Chem.* **2022**, *61*, 170–177. [CrossRef]
6. Zhao, M.; Liu, X.; Xu, X.; Liu, J. Ultrafast operation on a novel Nd:$LaMgAl_{11}O_{19}$ disordered crystal laser. *Infrared Phys. Technol.* **2022**, *124*, 104227. [CrossRef]
7. Wang, Z.; Liu, J.; Chen, P.; Liu, P.; Ma, J.; Xu, X.; Wei, Y.; Lebbou, K.; Xu, J. Growth and Characterization of Yb:CALYGLO Crystal for Ultrashort Pulse Laser Applications. *Crystals* **2024**, *14*, 120. [CrossRef]
8. Sun, L.; Lu, J.; Xu, Q.; Su, S.; Liu, R.; Lei, Z.; Xu, K.; Zou, Y.; Zhang, B.; Li, J.; et al. Crystal growth and spectral properties of a mixed crystal Nd^{3+}:$LuYPO_4$. *J. Lumin.* **2024**, *266*, 120297. [CrossRef]
9. Niu, X.; Chen, H.; Zhang, P.; Yin, H.; Hang, Y.; Li, Z.; Lin, W.; Chen, Z. Novel laser crystal Nd^{3+}: Ca(Y, Gd)AlO_4: A promising candidate for laser operation beyond 1.37 μm. *J. Alloys Compd.* **2023**, *938*, 168613. [CrossRef]
10. Wu, A.; Ding, J.; Xu, J.; Shen, H.; Ogawa, T.; Wada, S. Crystal growth and optical performance of Nd:$Sr_3Ga_2Ge_4O_{14}$ crystals. *Phys. Status Solidi A* **2008**, *205*, 1177–1180. [CrossRef]
11. Jiao, Y.; Liu, Z.; Zhang, X.; Gao, F.; Jia, C.; Chen, X.; Cong, Z. Diode-pumped actively Q-switched Nd:YVO_4/RTP intracavity raman laser at 1.49 μm. *Crystals* **2019**, *9*, 168. [CrossRef]
12. Xiao, H.; Zhao, T.; Ge, W.; Zhong, Q.; Li, M.; Yu, J.; Fan, Z.; Bian, S.; Chen, Y. High stability LED-pumped Nd:YVO_4 laser with a Cr:YAG for passive Q-switching. *Crystals* **2019**, *9*, 201. [CrossRef]
13. Liu, J.; Duan, Y.; Mao, W.; Jin, X.; Li, Z.; Zhu, H. An axicon-based annular pump acousto-optic Q-switched Nd:$GdVO_4$ self-raman vortex laser. *Crystals* **2023**, *13*, 1484. [CrossRef]
14. Zhang, Y.; Huang, C.; Xu, M.; Fang, Q.; Li, S.; Lin, W.; Deng, G.; Zhao, C.; Hang, Y. Nd:$GdScO_3$ crystal: Polarized spectroscopic, thermal properties, and laser performance at 1.08 μm. *Opt. Laser Technol.* **2023**, *167*, 109709. [CrossRef]
15. Chen, H.; Zhang, P.; Song, J.; Yin, H.; Hang, Y.; Yang, Q.; Li, Z.; Chen, Z. Spectral broadening of a mixed Nd:CYGA crystal with tunable laser operation beyond 1100 nm. *Opt. Express* **2022**, *30*, 21943–21951. [CrossRef] [PubMed]
16. Yuan, F.; Liao, W.; Huang, Y.; Zhang, L.; Sun, S.; Wang, Y.; Lin, Z.; Wang, G.; Zhang, G. A new ~1 μm laser crystal Nd:$Gd_2SrAl_2O_7$: Growth, thermal, spectral and lasing properties. *J. Phys. D Appl. Phys.* **2018**, *51*, 125307. [CrossRef]
17. Zhao, M.; Zhang, Z.; Feng, X.; Zong, M.; Liu, J.; Xu, X.; Zhang, H. High repetition rate passively Q-switched laser on Nd:SRA at 1049 nm with MXene $Ti_3C_2T_x$. *Chin. Opt. Lett.* **2020**, *18*, 21–24. [CrossRef]
18. Li, Y.; Jia, Z.; Nie, H.; Yin, Y.; Fu, X.; Mu, W.; Zhang, J.; Zhang, B.; Li, S.; Tao, X. Nd doped $CaYAl_3O_7$: Exploration and laser performance of a novel disordered laser crystal. *CrystEngComm* **2020**, *22*, 4723–4729. [CrossRef]
19. Zhang, T.; Zhou, L.; Zheng, W.; Xu, B.; Wang, Y.; Tu, C. Laser performance of diode-pumped continuous-wave Nd:$CaLaGa_3O_7$ laser with a 22-nm wavelength tunability. *Opt. Mater.* **2021**, *115*, 111022. [CrossRef]
20. Zhang, Y.; Zhang, S.; Gong, Q.; Fang, Q.; He, M.; Huang, C.; Li, S.; Zhang, X.; Xia, C.; Zhao, C.; et al. Structure and spectroscopic properties of a disordered Nd:$CaGdAl_3O_7$ crystal. *Infrared Phys. Technol.* **2023**, *131*, 104639. [CrossRef]
21. Liu, S.D.; Dong, L.L.; Zheng, L.H.; Berkowski, M.; Su, L.B.; Ren, T.Q.; Peng, Y.-D.; Hou, J.; Zhang, B.-T.; He, J.-L. High-power femtosecond pulse generation in a passively mode-locked Nd:$SrLaAlO_4$ laser. *Appl. Phys. Express* **2016**, *9*, 072701. [CrossRef]
22. Di, J.; Sun, X.; Xu, X.; Xia, C.; Sai, Q.; Yu, H.; Wang, Y.; Zhu, L.; Gao, Y.; Guo, X. Growth and spectral characters of Nd:$CaGdAlO_4$ crystal. *Eur. Phys. J. Appl. Phys.* **2016**, *74*, 10501. [CrossRef]
23. Li, D.Z.; Xu, X.D.; Cheng, S.S.; Zhou, D.H.; Wu, F.; Zhao, Z.W.; Xia, C.T.; Xu, J.; Zhang, J.; Zhu, H.M.; et al. Polarized spectral properties of Nd^{3+} ions in $CaYAlO_4$ crystal. *Appl. Phys. B-Lasers Opt.* **2010**, *101*, 199–205. [CrossRef]
24. Yang, H.; Jin, P.; Su, J.; Xu, X.; Xu, J.; Lu, H. Realization of a continuous-wave single-frequency tunable Nd: CYA laser. *Chin. Opt. Lett.* **2022**, *20*, 031403. [CrossRef]
25. Hontsu, S.; Ishii, J.; Kawai, T.; Kawai, S. $LaSrGaO_4$ substrate gives oriented crystalline $YBa_2Cu_3O_{7-y}$ films. *Appl. Phys. Lett.* **1991**, *59*, 2886–2888. [CrossRef]

26. Dabkowski, A.; Dabkowski, H.A.; Greedan, J.E. $SrLaGaO_4$-Czochralski crystal growth and basic properties. *J. Cryst. Growth* **1993**, *132*, 205–208. [CrossRef]
27. Ryba-Romanowski, W.; Gołąb, S.; Pisarski, W.; Dominiak-Dzik, G.; Gloubokov, A. Optical Study of $SrLaGaO_4$ and $SrLaGa_3O_7$ Doped with Nd^{3+} and Yb^{3+}. *Acta Phys. Pol. A* **1996**, *90*, 399–405. [CrossRef]
28. Zhang, Y.; Zhang, H.; Yu, H.; Sun, S.; Wang, J.; Jiang, M. Characterization of Disordered Melilite Nd:$SrLaGa_3O_7$ Crystal. *IEEE J. Quantum Electron.* **2011**, *47*, 1506–1513. [CrossRef]
29. Pan, Y.; Liu, B.; Liu, J.; Song, Q.; Xu, J.; Li, D.; Liu, P.; Ma, J.; Xu, X.; Lin, H.; et al. Polarized spectral properties and laser operation of Nd: $SrAl_{12}O_{19}$ crystal. *J. Lumin.* **2021**, *235*, 118034. [CrossRef]
30. Lomheim, T.S.; DeShazer, L.G. Optical-absorption intensities of trivalent neodymium in the uniaxial crystal yttrium orthovanadate. *J. Appl. Phys.* **1978**, *49*, 5517–5522. [CrossRef]
31. Dong, J.; Rapaport, A.; Bass, M.; Szipocs, F.; Ueda, K. Temperature-dependent stimulated emission cross section and concentration quenching in highly doped Nd^{3+}:YAG crystals. *Phys. Status Solidi A* **2005**, *202*, 2565–2573. [CrossRef]
32. Liu, Y.; Pan, F.; Gao, J.; Tu, C. Nd^{3+} doped $CaLaGa_3O_7$: Growth, structure, and optical properties of a disordered laser crystal. *J. Lumin.* **2022**, *244*, 118748. [CrossRef]
33. Zhang, Y.Y.; Zhang, H.J.; Yu, H.H.; Wang, J.Y.; Gao, W.L.; Xu, M.; Sun, S.Q.; Jiang, M.H.; Boughton, R.I. Synthesis, growth, and characterization of Nd-doped $SrGdGa_3O_7$ crystal. *J. Appl. Phys.* **2010**, *108*, 063534. [CrossRef]
34. Sato, Y.; Taira, T. Comparative study on the spectroscopic properties of Nd: $GdVO_4$ and Nd:YVO_4 with hybrid process. *IEEE J. Sel. Top. Quantum Electron.* **2005**, *11*, 613–620. [CrossRef]
35. Liu, S.; Dong, L.; Zhang, X.; Yao, Y.; Xu, Y.; Ren, T.; Zheng, L.; Su, L.; Berkowski, M. Thermal, spectral properties and Q-switched laser operation of Nd:$SrLaAlO_4$ crystal. *Opt. Mater.* **2017**, *64*, 351–355. [CrossRef]
36. Kushida, T.; Marcos, H.M.; Geusic, J.E. Laser transition cross section and fluorescence branching ratio for Nd^{3+} in yttrium aluminum garnet. *Phys. Rev.* **1968**, *167*, 289. [CrossRef]
37. Singh, S.; Smith, R.G.; Van Uitert, L.G. Stimulated-emission cross section and fluorescent quantum efficiency of Nd^{3+} in yttrium aluminum garnet at room temperature. *Phys. Rev. B* **1974**, *10*, 2566–2572. [CrossRef]